Available online at www.sciencedirect.com
SCIENCE DIRECT®
CRYOBIOLOGY
ELSEVIER
Cryobiology 52 (2006) 128–138
www.elsevier.com/locate/ycryo

Analysis of intracellular ice nucleation in *Xenopus* oocytes by differential scanning calorimetry ☆

F.W. Kleinhans [a,*,1], J.F. Guenther [a,b], D.M. Roberts [b], Peter Mazur [a,*]

[a] *Fundamental and Applied Cryobiology Group, Department of Biochemistry and Cellular and Molecular Biology, The University of Tennessee, Knoxville, TN 37932, USA*
[b] *Department of Biochemistry and Cellular and Molecular Biology, The University of Tennessee, Knoxville, TN 37996, USA*

Received 21 July 2005; accepted 26 October 2005
Available online 5 December 2005

Abstract

Intracellular ice formation (IIF) plays a central role in cell damage during cryopreservation. We are investigating the factors which trigger IIF in *Xenopus* oocytes, with and without aquaporin water channels. Here, we report differential scanning calorimeter studies of *Xenopus* control oocytes which do not express aquaporins. Stage I to VI oocytes (which increase progressively in size) were investigated with emphasis on stage I and II because they are translucent and can also be studied under the cryomicroscope. Measurements were made in 1, 1.5, and 2 M ethylene glycol (EG) in frog Ringers plus SnoMax. A multistep freezing protocol was used in which the samples were cooled until extracellular ice formation (EIF) occurred, partially remelted, slowly recooled through the EIF temperature, and then rapidly (10 °C/min) cooled. EIF in the 1, 1.5, and 2 M EG occurred at −6.4, −7.8, and −8.9 °C, respectively. Freezing exotherms of individual stage I–VI oocytes were readily visible. A general trend was observed in which the IIF temperature of the early stage oocytes (I–III) was well below T_{EIF} while the later stages (IV–VI) froze at temperatures much closer to T_{EIF}. Thus, in 1.5 M EG, T_{IIF} was −21.1, −25, and −26.6 °C in stages I–III, but was −17 and −8.5 °C for stage IV and V–VI. Concurrently, the percentage of oocytes in which IIF was observed fell dramatically from a high of 40 to 72% in early stages (I–III) to a low of only 7% in stage V–VI because, particularly in the later stages, IIF was hidden in the EIF exotherm. We conclude that early stage oocytes are a good model system in which to investigate modulators of IIF, but that late stage oocytes are damaged during EIF and infrequently supercool.

Keywords: Oocytes; *Xenopus*; DSC; Intracellular ice nucleation; IIF; Ethylene glycol

Intracellular ice formation (IIF) plays a central role in cell damage during cryopreservation. We are investigating the factors that trigger IIF in cells using mouse and *Xenopus* oocytes as a model. It has been hypothesized that membrane pores are an avenue for extracellular ice to trigger IIF [1,15] and that in some cells aquaporin channels may be those pores [17]. Mouse and *Xenopus* oocytes do

☆ This research was supported by NIH Grant R01-RR18470.
* Corresponding authors. Fax: +1 317 274 2393.
E-mail addresses: fkleinha@iupui.edu (F.W. Kleinhans), pmazur@utk.edu (P. Mazur).
[1] Present address: Department of Physics, Indiana University Purdue University Indianapolis, Indianapolis, IN 46202, USA.

0011-2240/$ - see front matter © 2005 Elsevier Inc. All rights reserved.
doi:10.1016/j.cryobiol.2005.10.008

not naturally express aquaporins but when injected with aquaporin complementary RNA, they are able to express aquaporin channels. This makes them an ideal model system in which to test these ideas.

Differential scanning calorimetry (DSC) has previously been used to study a number of comparably sized embryo systems. These include 13 h *Drosophila* embryos [21], 15–24 h *Anopheles* embryos [27], and several stages of zebrafish embryos [14]. In each case, the exotherms of individual embryo freezing events were readily observed. Thus, the technique is well established. Alternatively, bulk cell samples have also been studied with DSC, e.g., the investigation of IIF in human lymphocytes [2].

Our studies of *Xenopus* are proceeding in parallel with a cryomicroscope and with a DSC. Our cryomicroscope studies on mouse are reported by Mazur et al. [18]. Under the cryomicroscope, IIF is typically observed as a darkening or 'flashing' of the cells. In the DSC, IIF is 'observed' via the heat released by the individual oocytes on freezing. Here, we consider the *Xenopus* oocytes. They proceed through six stages of development (I–VI) during oogenesis in the ovary [7]. Traditionally, *Xenopus* stage V and VI oocytes are used as a model system in which to express genes and very little work has been done with early stage oocytes. However, in our work we wish to do parallel studies in a cryomicroscope and in a DSC. Translucent cells (stage I and II) are required to observe flashing under the cryomicroscope so we have emphasized them in these DSC studies, although not exclusively. Interestingly, the later stage oocytes proved more difficult to study because their freezing exotherms were often lost in the bulk media exotherm. We also report on some comparisons between the DSC and the cryomicroscope studies, showing good agreement between the two methods.

Materials and methods

Oocytes

Mature female oocyte positive *Xenopus laevis* frogs were obtained from *Xenopus* Express (Plant City, FL) and housed in tanks at the University of Tennessee, Knoxville animal facility. Oocytes were harvested as previously described [3] by surgical removal of oocyte sacks. Oocyte sacks were then defolliculated by treatment with 2 mg/ml collagenase type IA (Sigma No. C-9891) in filtered Ringers solution without calcium (96 mM NaCl, 2 mM KCl, 5 mM $MgCl_2$, and 5 mM Hepes–NaOH, pH 7.6) for 2–3 h at room temperature. Oocytes were periodically inspected visually during collaginase treatment to monitor follicular cell removal and to prevent over digestion [24]. Collaginase treatment was stopped by removal of collaginase by washing the oocytes in filtered Ringers solution (96 mM NaCl, 2 mM KCl, 5 mM $MgCl_2$, 0.6 mM $CaCl_2$, and 5 mM Hepes–NaOH, pH 7.6), and 100 μg/ml penicillin–streptomycin until the solution turned clear (usually 4–5 washes, 40 ml each). Oocyte stages were determined by size and appearance according to Hausen and Riebesell [7], Table 1, and separated into sterile 35 mm tissue culture dishes. Stage V and VI oocytes are not readily distinguished from each other and results for them have been grouped together in this report. Oocytes were cultured in filtered Ringers solution for 1–2 days at 16 °C before assay.

For DSC runs, oocytes were moved to a small Petri dish containing the desired test solution, namely 1.0, 1.5, or 2.0 M ethylene glycol (EG) in frog Ringers (210 mosm) containing 10 mg/L of Pseudomonas syringae (SnoMax, York International, Victor, NY) as an ice nucleating agent.

Table 1
Xenopus oocyte developmental stages[a]

Stage	I	II	III	IV	V[d]	VI[d]
Diameter (μm)	50–300[b]	300–450	450–600	600–1000	1000–1200	1200–1300
Appearance	Transparent	White, Translucent[c]	Opaque, light brown, yolk buildup begins	Opaque, animal vegetal pigmentation appears	Opaque, hemispheres clearly delineated (dark brown light yellow)	Opaque, hemispheres clearly delineated

[a] After Hausen and Riebesell [7].
[b] We limited our study of stage I oocytes to the size range from ~200 to 300 μm in diameter.
[c] Stage 2 is generally described as opaque, however, we find it sufficiently translucent to detect the presence of IIF via dark, ice flashing.
[d] Stage V and VI oocytes can not be readily distinguished from each other and are grouped together in this study.

The oocytes were allowed 5–10 min for equilibration and then transferred to a DSC sample pan. A transfer volume of 4 μl (oocytes and media) was used and contained one to ten oocytes depending on stage (8–10, stage I; 4, stage III or IV; and 1–2, stage V or VI). After crimping a lid on the sample pan, it was moved immediately to the DSC head and after a few minutes DSC equilibration time, the thermal run begun. The DSC thermograms often exhibited a small secondary water freezing peak. The size of this peak was found to depend on the delay time between sample pan crimping and the freezing run. We attribute this peak to water which evaporated from the sample droplet and recondensed elsewhere in the sample pan.

DSC

A Perkin–Elmer (PE) DSC-7 differential scanning calorimeter and PE Thermal Analysis Software, Ver. 2.20, running under a Unix operating system, a PE Liquid Nitrogen Subambient Accessory, and PE crimpable aluminum sample pans (#0219–0062) were used for all the DSC experiments. The DSC was calibrated at the beginning of these experiments per the PE manual using cyclohexane which has phase transitions at 6.54 and −87.06 °C. The calibrations were done with a sweep rate of +10 °C/min; i.e., in warming mode as required by the calibration procedure, to avoid supercooling problems. Thus, the DSC calibration only holds for a sweep rate of +10 °C/min. However, the experiments reported here were done in cooling mode with sweep rates of −4 to −10 °C/min. Because of thermal lag in the DSC, it is necessary to apply a correction factor [2,8,19]. In a series of thermal lag experiments, the melting point of water and of 1.5 M EG in frog Ringers was measured at scan rates of +0.5 to +20 °C/min (Fig. 1). In a similar series of experiments, the freezing point of 1.5 M EG in frog Ringers with 10 mg/L SnoMax was measured at scan rates of −0.5 to −20 °C/min. From these data, the temperature correction (T_C) to the raw DSC temperatures, for a given cooling rate (CR), was determined to be:

$$T_C = 0.6°C + (10°C/\,\mathrm{min})(0.175\,°C/°C/\,\mathrm{min}) + (\mathrm{CR})(0.11\,°C/°C/\,\mathrm{min}).$$

The three terms in this equation bear some explanation. After the cyclohexane calibration of the DSC, a residual error of 0.6 °C in the melting point of water was found and we prefer to correct this small error in 'software' rather than constantly readjusting the DSC, thus the first term. The second and third terms correct for thermal lag in the DSC. For instance, at a scan rate of −4 °C/min the actual scan rate (−4 °C/min) and calibration scan rate (+10 °C/min) differ by 14 °C. The lag correction has to account for this 14 ° span. Empirically, we find a different lag correction (0.175 °C/ °C/min) for the positive portion of this span (+10–0 °C/min) than for the negative portion of this span

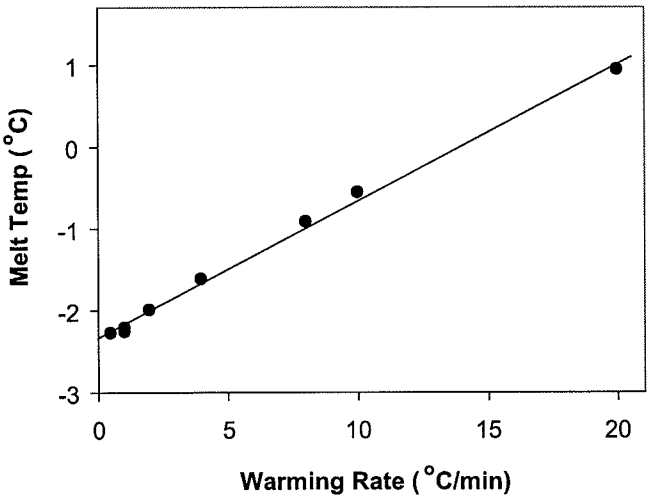

Fig. 1. Effect of DSC scan rate on measured onset melting point of water. Our DSC was calibrated at a warming rate of 10 °C/min. At other scan rates, a thermal lag correction factor must be applied to measured temperatures. The data above yield a lag correction factor of +0.168 °C/(°C/min), from the slope, and the temperature offset at 10 °C/min yields a residual calibration error of −0.67 °C. Considering all of the warming rate data yields a lag correction of 0.175 °C/(°C/min) and a residual calibration error of −0.6 °C.

(0 to −4 °C/min), where the lag correction is 0.11 °C/ °C/min. Thus, a CR of 4 °C/min differs from the calibration rate by 14 °C and yields the following terms in the TC equation: (1) 0.6 °C residual calibration correction, (2) a correction applicable to the span 10 to 0 °C/min of (10 °C/min) * (0.175 °C/ °C/min) = 1.75 °C, and (3) a correction applicable to the span 0 to -4 °C/min of (4 °C/ min) * (0.11 °C/ °C/min) = 0.44 °C. Summing these terms yields a TC of +2.8 °C which was applied to all the DSC temperatures measured at a scan rate of −4 °C/min. In a similar fashion, the correction for scans done at −10 °C/min is found to be +3.5 °C. Our DSC software dates from 1994. Newer systems may automatically correct for some of these lag effects, but these corrections should always be verified.

The oocyte cooling protocol was set up in a fashion similar to that used in our Linkam cryomicroscope studies of mouse oocytes [18]. Specifically, the sample is: (1) cooled rapidly from room temperature to just above the extracellular ice formation (EIF) temperature, (2) cooled slowly through the EIF freezing transition, (3) warmed slowly to just below the melting point (to melt most of the ice), (4) re-cooled slowly for several degrees to slowly refreeze most of the aqueous media, and (5) cooled at 10 °C/min to −50 °C. It is during this last cooling ramp that the intracellular ice formation (IIF) is typically detected. In some cases, IIF is seen before this final cooling ramp, as will be discussed later. Figs. 2A and B illustrate the thermal protocol for the 1.5 M EG solutions. In the 1 and 2 M EG solutions, the ramp transition points are adjusted up and down as needed to account for the different T_{EIF} and melting point of these solutions. Fig. 3A illustrates some typical IIF exotherms occurring in ramp 5. The purpose of the ramps 2, 3, and 4 is to seed the sample and then to begin the freezing process slowly so that the oocytes are sequestered in a matrix of slowly growing ice. In our mouse oocyte work with a Linkam cryomicroscope, this is found to be less damaging to the oocytes then sequestering them in an ice matrix produced by rapid freezing after supercooling [18].

Occasionally, it is desirable to quantify the heat released during oocyte freezing. This requires determining the area under one of the IIF peaks, Fig. 3A. The area will have units of the product of the X and Y axes. The X axis is actually a time axis which the PE software automatically converts to temperature based on the sweep rate. Thus, the area units are:

$$X * Y = (\Delta T/\text{Swp\_Rate}) * (\text{mW}) = (^\circ\text{C}/(^\circ\text{C/s})) * (\text{mJ/s}) = \text{mJ},$$

a unit of energy or heat release. The PE software can compute these areas (energies), but to a good approximation, these simple peaks (Fig. 3A) are just triangles for which the area is given by 1/2 * base * - height. For stage I to IV oocytes, we empirically found the base width to be constant. Thus, the height of a freezing exotherm is proportional to the energy in the exotherm. Occasionally two oocytes freeze at the same temperature and in this case a peak of double height is obtained (and easily recognized).

Modeling oocyte response to EG solutions

The oocyte response to the EG test solutions was modeled to estimate their volume and internal EG concentration after 8–12 min of equilibration. Standard two-parameter modeling techniques were used [10]. The hydraulic conductivity, Lp, in the presence of EG was taken to be 0.35 μm/min/ atm; half its value in the absence of CPA [23]. The EG permeability, Ps, was taken to be 0.001 cm/min [4]. Finally, the inactive cell volume was taken to be 0.7 in stage V and VI [4] and 0.15 in stage I and II [11].

Results

Detection of IIF and EIF

The freezing of individual stage I to VI oocytes is readily detected in the DSC-7. In total, 103 DSC runs examining 450 oocytes were conducted yielding 236 IIF peaks. An example of the freezing of single stage II oocytes is depicted in Fig. 3A. In this particular run, 10 oocytes were in the sample pan, with eight yielding IIF peaks. Stage I oocytes have peaks only one quarter as large, but these are still well above the noise level. Two checks were made to verify that these peaks are oocyte IIF peaks. First, the area under the peaks should increase proportionately with the size (stage) of the oocytes. As a practical matter, we used peak height as a proxy for peak area as justified in Materials and methods. Two uncertainties affect this height–size comparison. First, each oocyte stage, identified on the basis of appearance, exhibits a range of sizes (Table 1). Second, the oocyte water volume depends on the fraction of the cell, which is water, namely (1 − Vb)

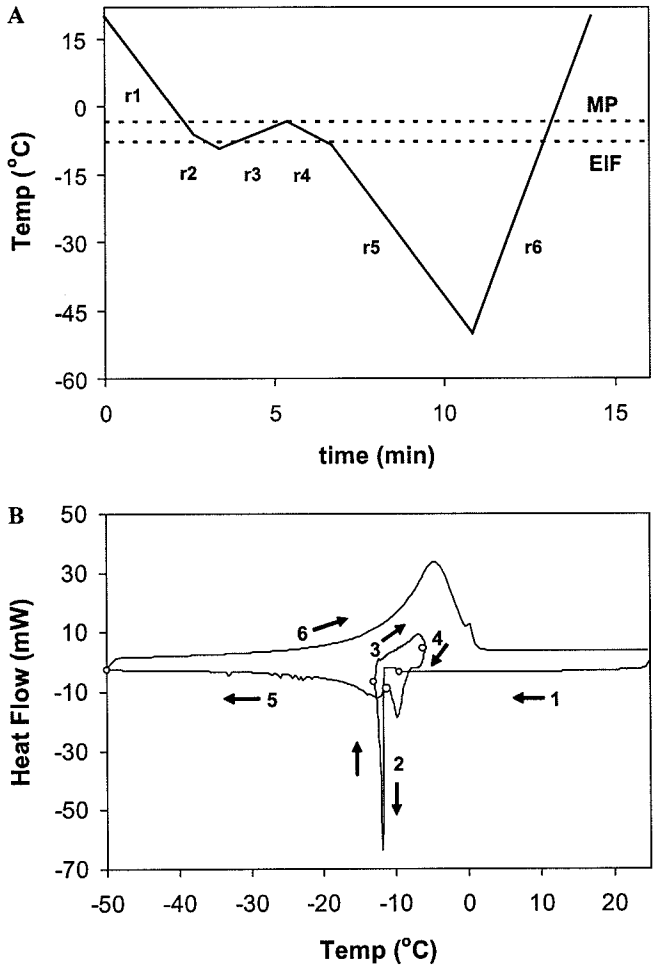

Fig. 2. (A) Thermal ramp protocol for oocytes in 1.5 M EG in frog Ringers with SnoMax. The top dotted line is the melting point of the solution (1.85 osmolal, −3.44 °C melting point) and the bottom is the average EIF temperature (−7.8 °C). The cycle from ramp 2 to ramp 4 is designed to seed, nearly remelt, and then freeze the sample at an initial slow rate. The ramp rates are: ramp 1, −10 °C/min; ramp 2 and 4, −4 °C/min; ramp 3, +4 °C/min; ramp 5, −10 °C/min; ramp 6, +20 °C/min. In 1 and 2 M EG solutions the ramp transition points are shifted up and down, accordingly, to account for the different solution EIF's and melting points. (B) DSC thermogram showing the thermal protocol for stage II oocytes in 1.5 M EG/Ringers. The ramp transitions are denoted by open circles. The sharp down peak at −12 °C is the initial, rapid freezing of the supercooled media. During ramps 3 and 4 the sample is partially melted and slowly refrozen. The broad peak around −4 °C in ramp 6 is the final melting of the sample during return to room temperature. Anytime there is a change in cooling/warming rate there is a shift in the thermogram baseline for several seconds. This is obvious at −50 °C where the rate changes from −10 to +20 °C/min. On closer examination, a shift can be seen at every ramp transition. The temperatures shown are raw, uncorrected DSC readout temperatures. See the text for thermal lag corrections.

where Vb is the osmotically inactive fraction of the cell contents. In permeability experiments, we determined Vb to equal 0.15 in stage I and II oocytes [11] and Edashige [4] found Vb to equal 0.7 in Stage VI oocytes (consistent with the accumulation of large stores of yolk beginning at stage III [7]). For the unmeasured stage III and IV oocytes, we assume intermediate Vb's of 0.2 and 0.4. These data are collected in Fig. 4 and show a good correlation between peak height and estimated oocyte water volume.

A second check of the IIF peak authenticity is to compare the actual heat release in a peak with that theoretically expected from the latent heat of fusion of water. This was done for several stage II oocytes and gave agreement within a factor of 2. This discrepancy likely results from uncertainties in the oocyte volume, since they were picked on the basis of visual stage appearance, and not measured size. The above two observations, as well as the fact that the number of putative IIF peaks was always less than or equal to the number of oocytes in the

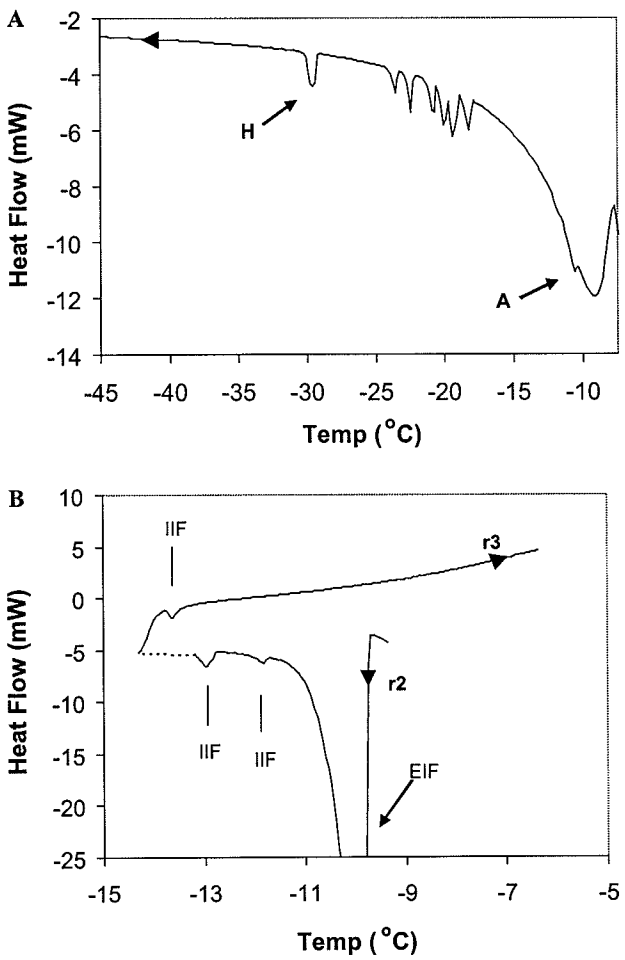

Fig. 3. (A) Eight IIF peaks of stage II oocytes (A to H). The sample contained 10 oocytes in 1.5 M EG in frog Ringers with SnoMax. This is a magnification of the ramp 5 cooling thermogram shown in Fig. 2B. Peak A appears on the low side of the bulk media freezing peak and the rest occur at progressively lower temperatures. All these peaks are referred to as low IIF peaks. The above temperatures are true temperatures and have been corrected from Fig. 2B by a calibration and scan correction of +3.5 °C; see text. (B) Typical example of oocyte IIF peaks that occur in ramps 2 (cooling from −9 to −14 °C) and 3 (warming from −14 to −6 °C), which are referred to as high IIF peaks. Two peaks appear in ramp 2, just after EIF has occurred, and one peak appears in ramp 3 during sample rewarming. These are stage III oocytes in 2 M EG. The dotted line connecting ramp 2 and 3 is an inevitable consequence of changing the heating/cooing rate and, therefore, the thermal lag correction. Essentially, the temperature is not well known during a change in cooling/heating rate. Otherwise, the temperatures have been fully corrected for thermal lag effects.

sample (down to zero), persuaded us that we were observing the freezing of individual oocytes.

The extracellular ice formation temperature is taken as the beginning of the sharp down peak in the thermograms during the ramp 2 cooling. In Fig. 2B, it occurs at −11.7 °C (uncorrected temperature).

EIF temperature

The EIF temperatures range from −6.4 to −8.9 °C in 1–2 M EG, respectively (Table 2). By using an ice nucleator, SnoMax, EIF can be induced at relatively high and reproducible temperatures. As expected, solutions with a higher EG concentration have a lower EIF temperature.

IIF peaks seen and not seen

We start with a key point: the fraction of the oocytes in a sample that exhibit an IIF peak is highly stage dependent. For early stage oocytes (I–III), the percentage detected is 40–72%. However, by stage V and VI the percentage seen drops to 7% (Fig. 5). Thus, 93% of the oocytes are *undetected*

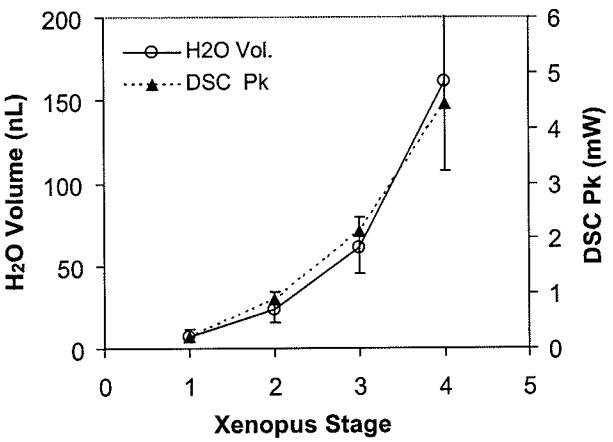

Fig. 4. Comparison of DSC peak heights (solid triangles) in milliwatts with estimated oocyte aqueous volume (open circles) as a function of oocyte stage. Technically, the oocyte water volume should be compared with the energy (area) of the DSC peaks. However, because several factors including scan rate and base width of the peaks are constant, good correlation is found between the height of the DSC thermogram peaks and the estimated oocyte water volume as a function of stage. The inactive, non-water, cell volume at each stage is estimated to be 0.15, 0.15, 0.2, and 0.4 for stages I–IV, respectively (see text). Because only correlation is being demonstrated, the left and right graphs were adjusted up and down for best overlap. The error bars are for the volume range of each stage, Table 1. Data are for a representative number of samples (33 total).

Table 2
EIF as a function of ethylene glycol concentration

EG (M)	EIF (°C)	SEM (°C)	*N* #
1.0	−6.4	0.2	19
1.5	−7.8	0.1	86
2.0	−8.9	0.1	37

The EG is dissolved in frog Ringers with an osmolality of 210 mosm and containing SnoMax (10 mg/L).

at this stage, presumably because their exotherms are lost in the bulk exotherm at EIF.

The IIF peaks seen are divided into two groups. The first comprises those which occur during rapid cooling (10 °C/min), after the sample has first been seeded, rewarmed, and slowly refrozen to just below the EIF temperature. These are referred to as the low IIF group. They cool to below the EIF temperature and freeze in ramp 5 (Fig. 3A) at temperatures of 0.7–37 °C below T_{EIF}. Up to stage IV, the majority of IIF peaks seen are in this group. The second group comprises those which freeze during the initial seeding freeze or rewarming (ramps 2 or 3) at temperatures near T_{EIF} and before ramp 5 is reached. These are referred to as the high IIF group, e.g., Fig. 3B. By stage V and VI, those few IIF peaks which are seen, typically belong to this group. This will be discussed further below and in Discussion.

IIF temperature vs stage and EG concentration

As noted above, the oocytes fall into two groups: those which freeze during their passage through EIF, the high IIF group, and those which pass through EIF and freeze during rapid cooling in ramp 5, the low IIF group. The T_{IIF} results for both groups as a function of stage are shown in Fig. 6. Several trends are apparent.

Low IIF group

Among the low IIF group oocytes, there is a general trend for IIF to occur at higher temperatures as the development stage increases, so that by stage V and VI, nearly all the oocytes freeze just below T_{EIF}. For example, in 1.5 M EG, IIF occurs at −25.0, −17.0, and −8.5 °C in stage II, IV, and V–VI oocytes, respectively, while EIF occurs at −7.8 °C.

The effects of CPA concentration on T_{IIF} in the low IIF group are clearly seen in the stage I and II data, summarized in Table 3. T_{IIF} ranges from −18.6 to −35.2 °C with the depression systematically increasing with increased EG concentration. This decrease in T_{IIF} as a function of cryoprotectant concentration is similar to that observed in other cells such as *Drosophila* embryos [21], mouse embryos [25], and mouse oocytes [18].

High IIF group

In the high IIF group, by definition, all the oocytes freeze near their respective EIF temperatures, which decreases slightly as the EG concentration increases (Fig. 6). As noted previously, few oocytes freeze in the high IIF group. The total number of high group freezers shown in Fig. 5 is 18, compared with 218 in the low IIF group.

Unseen group

We stress once again, that not all the oocytes are observed to freeze, especially for the later stage oocytes. The percent unseen is just (100%–% seen, Fig. 5) and ranges from a low of 28% at stage III to a high of 93% unseen at stage V–VI. We presume the unseen oocytes freeze during EIF and are lost in the bulk exotherm.

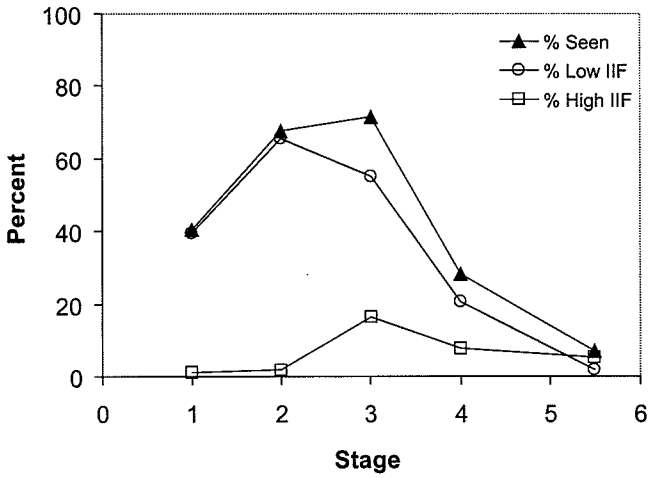

Fig. 5. Percent of oocytes observed to freeze as a function of stage (solid triangles). These freezing peaks are divided into two groups of oocytes, those which were observed to freeze below the EIF temperature in ramp 5, the low IIF group (open circles), and those which were observed to freeze near the EIF temperature in ramps 2 and 3, the high IIF group (open boxes). Some 40–65% of early stage oocytes (I–III) cool well below T_{EIF} and their freezing peaks are well separated from the bulk freezing of the solution, making them readily visible. However, by stage V and VI, very few oocyte peaks are seen, presumably because the remaining, unseen, oocytes are freezing concurrently with EIF and are typically 'lost' in the bulk solution peak.

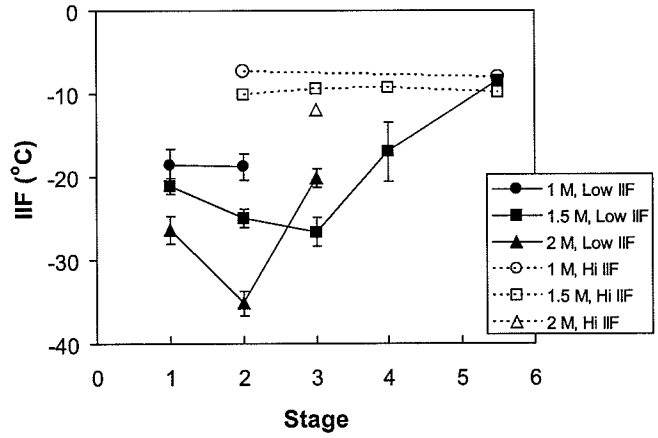

Fig. 6. Oocyte IIF temperature as a function of stage. The data fall into two groups. The first is comprised of those oocytes (solid symbols) which freeze in cooling ramp 5 below the EIF temperature. These are referred to as the low IIF group because their freezing occurs after the sample has been seeded, warmed, and slowly refrozen to below the EIF temperature. The second group comprises those oocytes (open symbols) which freeze during the initial seeding freeze or rewarming (ramps 2 and 3) near the EIF temperature. This group is referred to as the high IIF group. Circles, squares, and triangles refer to oocytes in 1.0, 1.5, and 2.0 M EG solutions, respectively. Some 40–65% of stage (I–III) oocytes show distinct IIF peaks well below EIF, Fig. 5. For later stage oocytes (V–VI), the mean IIF temperature approaches EIF where most of the peaks are lost in the bulk solution freezing peak. SEM error bars are shown for the low IIF group for which N/(data point) ranges from 8 to 59 (with the exception of stage 5.5 in 1.5 M EG for which $N = 1$). In the high IIF group, N averages two and ranges from 1 to 7, so no error bars are shown.

Comparison with cryomicroscope data

Xenopus stage I and II oocytes are of particular importance to our research program because their IIF can also be observed under the cryomicroscope via flashing. Parallel studies in our laboratory of *Xenopus* oocytes in a Linkam cryomicroscope, using similar cooling ramps, are nearing completion [5]. Comparison of the solution EIF temperatures and combined stage I and II IIF data are shown in Fig. 7. Both the EIF and IIF temperatures are in good agreement between the two methods.

Table 3
Comparison of T_{IIF} as a function of EG concentration in several cell types

Cell (type)	Water volume (nl)	Cooling rate (°C/min)	T_{IIF}		
			1 M EG (°C)	1.5 M EG (°C)	2 M EG (°C)
Xenopus stage I oocyte[a]	≈6.9	−10	−18.6 ± 1.9	−21.1 ± 1.0	−26.4 ± 1.7
Xenopus stage II oocyte[a]	≈23	−10	−18.8 ± 1.6	−25.0 ± 1.1	−35.2 ± 1.4
Permeabilized *Drosophila* embryo (13 h)[b]	5.4	−4	−23	−27	−33
Mouse oocyte[c]	≈0.18	−20	−37.2	−40.8	—

[a] This work. Average ± SEM.
[b] Myers et al. ([21], Fig. 3).
[c] Mazur et al. [18].

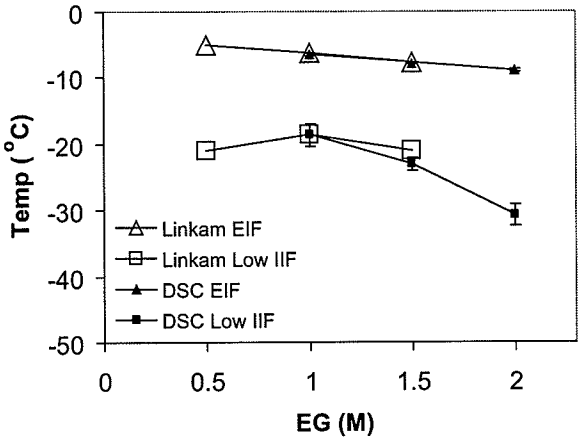

Fig. 7. Comparison of DSC and Linkam cryomicroscopy EIF and *Xenopus* oocyte IIF data as a function of EG concentration. (triangles, EIF; squares, IIF; closed symbols, DSC; open symbols, cryomicroscope). DSC data for low IIF group stage I and II have been combined for comparison with the cryomicroscopy stage I and II low IIF data; SEM error bars. The agreement between the two methods is excellent.

Discussion

First, we consider the state of the oocytes in the ethylene glycol test solutions. Oocytes were held for 8–12 min prior to initiating a DSC scan and during this time they exhibited a shrink-swell response with shrinkage seen as a dimpling of the oocytes. Based on modeling the response of the embryos (see Materials and methods) we estimate that they may be shrunken by 10–30% in volume but are nearly equilibrated to the external EG concentration at the beginning of DSC runs. The 8–12 min equilibration time was a compromise between allowing time for full equilibration (60 min) and minimizing the time for solution damage. We do not believe this modest volume shrinkage appreciably affects our results.

The Perkin-Elmer DSC-7 has the necessary sensitivity to observe the freezing, via latent heat of fusion, of individual eggs at all stages, I to VI, of *Xenopus* oocytes with water volumes ranging from approximately 6.9 to 240 nl. This is not an unexpected result as DSC has previously been used to study the freezing of individual embryos with comparable water volumes, including *Drosophila*, 5.4 nl [21], Anopheles, 3.5 nl [27], and zebrafish embryos, 90 nl [14].

What is surprising is that IIF of the late stage *Xenopus* oocytes (V and VI) was largely unobservable, Fig. 5. The likely explanation for this is that their freezing was obscured by the large exotherm of EIF in the external solution which occurs at −6.4 to −8.9 °C depending on the EG concentration. We believe that virtually all the stage V and VI oocytes are damaged during EIF. Most freeze immediately upon damage and their IIF freezing exotherm is lost in the bulk media exotherm. However, we believe a small percentage exhibit a short lag before the damage leads to freezing. This would explain the high IIF group in which IIF is observed to occur temporally just after EIF, either just below the EIF temperature or during the rewarming in ramp 3 (Fig. 3B).

Similar high IIF temperatures have been observed in some other large oocyte and embryo systems. Koseoglu et al. [13] found, using cryomicroscopy, that starfish oocytes ($d = 170$–200 μm) experienced IIF within 3 °C of T_{EIF} in both isotonic media and in 1.5 M Me_2SO. In zebrafish embryos ($d \approx 700$ μm), Hagedorn et al. [6] found, using cryomicroscopy, that T_{IIF} occurred at the same temperature as T_{EIF} in isotonic embryo medium and in embryo medium plus 1 M propylene glycol. Liu et al. [14] have also studied zebrafish embryos, in their case using DSC. In these latter studies, the embryos were suspended in oil rather than aqueous media and, as they note, their results provide some insights into the possible

mechanisms at work in IIF. At the 6-somite stage, with chorion intact, T_{IIF} for embryos in oil is −11.9 °C [14], while T_{IIF} occurs at a comparable −14.2 °C for embryos in embryo medium [6]. However, when the embryos are dechorinated (and the perivitaline fluid removed), the embryos suspended in oil do not freeze until −23.5 °C and after treatment with 2 M methanol, T_{IIF} is suppressed an additional 4.3 °C [14]. As noted by these authors [6,14], these data suggest that extracellular ice plays a key role in triggering IIF and when this extracellular ice formation is prevented (by placing dechorinated embryos in oil to remove external water), IIF occurs at a much lower temperature.

It is generally assumed that contact between extracellular ice and cells is a necessary, but not sufficient condition, for heterogeneous nucleation of IIF [9,17,20,22]. We speculate that the high IIF temperature we observe for late stage (V and VI) *Xenopus* oocytes is related to their large size which increases the probability for cell–ice contact. When cells freeze in media, they are sequestered in the unfrozen channels as the freezing proceeds [16,26]. Larger cells will make contact and be deformed by these channels at a higher temperature than small cells. In a companion paper to this on cryomicroscopy studies of mouse control oocytes, Mazur et al. [18] discuss a number of the issues potentially affecting IIF such as the composition and unfrozen fraction of the media at the time of IIF.

As previously discussed, we are primarily interested in the smaller, translucent, stage I and II oocytes. These oocytes typically survive their passage through EIF, and IIF occurs well below the melting temperature of the respective solutions and is correlated with increased CPA concentration. This is a typical behavior for IIF in cells as a function of CPA concentration as illustrated by similar results in *Drosophila* and mouse oocytes (Table 3). In 13 h, permeabilized *Drosophila* embryos, of comparable size to stage I *Xenopus* oocytes, IIF occurs at −23 to −33 °C in 1–2 M EG solutions [21], while the corresponding IIF temperatures for *Xenopus* are −18.6 to −26.4 °C.

Our long term objective is to use these early stage *Xenopus* oocytes as a model system for examining the effect on T_{IIF} of introducing pores, e.g., aquaporins into the cell membrane. Our hypothesis is that IIF is caused by extracellular ice nucleating IIF and that introducing pores will increase the efficacy of this process, causing it to happen at a higher temperature. To be a good model system, the *Xenopus* control oocytes should undergo substantial supercooling so that even small perturbations of the IIF process by aquaporins will show up as an increase in T_{IIF}. On this basis, we believe that early stage *Xenopus* oocytes are a good model system as illustrated in Table 4 which shows supercooling at IIF of 16.2–30.5 °C for stage I and II oocytes in 1–2 M EG.

For several reasons, we believe stage II oocytes will prove a better model system than stage I. They subjectively seem more robust during handling, yield a larger DSC exotherm on freezing, and provide a larger image for microscopy. The relatively greater fragility of the stage I oocytes may explain why they supercool somewhat less than stage II. If they are more fragile, the stage I oocytes may be more easily damaged as they become imbedded in the ice matrix on solution freezing, thus permitting entry of extracellular ice and subsequent triggering of IIF.

In our laboratory, we are examining *Xenopus* oocytes using both DSC and cryomicroscope. To be effective and readily interpretable it is desirable that the DSC and cryomicroscope yield similar results when similar solution or oocyte properties are measured. As shown in Fig. 7, the solution EIF data show excellent temperature agreement between the DSC and cryomicroscope. Indeed, the nearly exact EIF agreement is likely fortuitous as our DSC calibration procedures are probably only

Table 4
Supercooling[a] of *Xenopus* oocytes at their IIF temperature in ethylene glycol solutions

EG (M)	T_{melt}[b] (°C)	Stage I		Stage II	
		T_{IIF} (°C)	$T_{melt} - T_{IIF}$ (supercooling) (Δ °C)	T_{IIF} (°C)	$T_{melt} - T_{IIF}$ (supercooling) (Δ °C)
1.0	−2.4	−18.6	16.2	−18.8	16.4
1.5	−3.5	−21.1	17.6	−25.0	21.5
2.0	−4.7	−26.4	21.7	−35.2	30.5

[a] The degree of supercooling is computed as the difference between the solution melting temperature and T_{IIF}. The oocytes are assumed to have equilibrated with the external EG solution. If they have not, the supercooling may be slightly greater.
[b] The melting temperature is the freezing point depression computed as 1.86 °C times the osmolality of the solution.

accurate to several tenths of a degree. The (combined) stage I and II IIF data also show good agreement. We believe this demonstrates, as desired, that the freezing behavior of the oocytes is determined by the properties of the oocytes and their interactions with the external medium rather than the characteristics of the sample container geometry or volume which differ appreciably between the two instruments. Similarly, the freezing properties, T_{EIF}, of the medium is independent of instrumental differences. Similar agreements between DSC and cryomicroscopy studies have been obtained by Korber et al. [12] for human lymphocytes.

In summary, differential scanning calorimetry has proven an effective way to measure IIF in *Xenopus* oocytes and demonstrates that early stage oocytes are a useful model system for investigating IIF. Also, DSC and cryomicroscopy results are comparable for stage I and II. The next step in our work is to examine oocytes expressing aquaporins.

Acknowledgments

We thank several people for their assistance with this project. Ian Wallace performed some of the frog surgeries. Irina Pinn and Seki Shinsuke helped with some of the sample preparations. Finally, Keisuke Edashige assisted with some of the preliminary DSC measurements on Stage V–VI oocytes.

References

[1] J.P. Acker, J.A.W. Elliott, L.E. McGann, Intercellular ice propagation: experimental evidence for ice growth through membrane pores, Biophys. J. 81 (2001) 1389–1397.
[2] G. Bryant, DSC measurement of cell suspensions during successive freezing runs: implications for the mechanisms of intracellular ice formation, Cryobiology 32 (1995) 114–128.
[3] R.M. Dean, R.L. Rivers, M.L. Zeidel, D.M. Roberts, Purification and functional reconstitution of soybean nodulin 26: an aquaporin with water and glycerol transport properties, Biochemistry 38 (1999) 347–353.
[4] K. Edashige, Personal communication, College of Agriculture, Kochi University, Nankoku, Kochi 783–8502, Japan, e-mail: keisuke@cc.kochi-u.ac.jp.
[5] J. Guenther, D. Roberts, P. Mazur, A study of extra-and intracellular ice formation in *Xenopus* eggs by cryomicroscopy, Cryobiology 51 (3) (2005), [Abstract 111].
[6] M. Hagedorn, A. Peterson, P. Mazur, F.W. Kleinhans, High ice nucleation temperature of zebrafish embryos: slow-freezing is not an option, Cryobiology 49 (2004) 181–189.
[7] P. Hausen, M. Riebesell, The Early Development of *Xenopus laevis*, Springer-Verlag, New York, 1991.
[8] H.-J. Hinz, F.P. Schwarz, Measurement and analysis of results obtained on biological substances with differential scanning calorimetry (IUPAC Technical Report), Pure Appl. Chem. 73 (2001) 745–759.
[9] J.O.M. Karlsson, E.G. Cravalho, M. Toner, Intracellular ice formation: causes and consequences, Cryo-Letters 14 (1993) 323–334.
[10] F.W. Kleinhans, Review: membrane permeability modeling: Kedem–Katchalsky vs. a two-parameter formalism, Cryobiology 37 (1998) 271–298.
[11] F.W. Kleinhans, J.F. Guenther, S. Seki, K. Edashige, D.M. Roberts, P. Mazur, Water P_f of Xenopus (AQP1±) stage I and II oocytes, Cryobiology 51 (3) (2005), [Abstract 110].
[12] C. Korber, S. Englich, G. Rau, Intracellular ice formation: cryomicroscopic observation and calorimetric measurement, J. Microsc. 161 (1991) 313–325.
[13] M. Koseoglu, M. Toner, K.C. Sadler, A. Eroglu. Starfish oocytes form intracellular ice at unusually high temperatures, Cryobiology 43 (2001) 248–259.
[14] X.-H. Liu, T. Zhang, D.M. Rawson, Differential scanning calorimetry studies of intraembryonic freezing and cryoprotectant penetration in zebrafish (*Danio rerio*) embryos, J. Expt. Zool. 290 (2001) 299–310.
[15] P. Mazur, The role of cell membranes in the freezing of yeast and other cells, Ann. NY Acad. Sci. 125 (1965) 658–676.
[16] P. Mazur, W.F. Rall, N. Rigopoulos, Relative contributions of the fraction of unfrozen water and of salt concentration to the survival of slowly frozen human erythrocytes, Biophys. J. 36 (1981) 653–675.
[17] P. Mazur, Principles of cryobiology, in: B.J. Fuller, N. Lane, E.E. Benson (Eds.), Life in the Frozen State, CRC Press, Boca Raton, 2004, pp. 3–65.
[18] P. Mazur, S. Seki, I.L. Pinn, F.W. Kleinhans, K. Edashige, Extra- and intracellular ice formation in mouse oocytes, Cryobiology 51 (2005) 29–53.
[19] J.L. McNaughton, C.T. Mortimer, Differential Scanning Calorimetry, IRS Physical Chemistry Series 2, vol. 10, Butterworths, London, 1975. Reprinted by Perkin-Elmer, # L-604.
[20] J.A. Mugnano, T. Wang, J.R. Layne Jr., A.L. DeVries, R.E. Lee Jr., Antifreeze glycoproteins promote intracellular freezing of rat cardiomyocytes at high subzero temperatures, Am. J. Physiol. 269 (1995) R474–R479.
[21] S.P. Myers, R.E. Pitt, D.V. Lynch, P.L. Steponkus, Characterization of intracellular ice formation in *Drosophila melanogaster* embryos, Cryobiology 26 (1989) 472–484.
[22] R.E. Pitt, P.L. Steponkus, Quantitative analysis of the probability of intracellular ice formation during freezing of isolated protoplasts, Cryobiology 26 (1989) 44–63.
[23] G.M. Preston, T.P. Carroll, W.B. Guggino, P. Agre, Appearance of water channels in *Xenopus* oocytes expressing red cell CHIP28 protein, Science 256 (1992) 385–387.
[24] M.W. Quick, H.A. Lester, Methods for expression of excitability proteins in *Xenopus* oocytes, Methods Neurosci. 19 (1994) 261–279.
[25] W.F. Rall, P. Mazur, J.J. McGrath, Depression of the ice-nucleation temperature of rapidly cooled mouse embryos by glycerol and dimethyl sulfoxide, Biophys. J. 41 (1983) 1–12.
[26] G.L. Rapatz, L.J. Menz, B.J. Luyet, Anatomy of the freezing process in biological materials, in: H.T. Meryman (Ed.), Cryobiology, Academic Press, New York, 1966, pp. 139–162.
[27] P.D. Schreuders, E.D. Smith, K.W. Cole, M.-D.-P. Valencia, A. Laughinghouse, P. Mazur, Characterization of intraembryonic freezing in *Anopheles gambiae* embryos, Cryobiology 33 (1996) 487–501.